Carbohydrate Polymers 156 (2017) 34–44

Contents lists available at ScienceDirect

Carbohydrate Polymers

journal homepage: www.elsevier.com/locate/carbpol

Effect of microwave argon plasma on the glycosidic and hydrogen bonding system of cotton cellulose

S. Prabhu*, K. Vaideki, S. Anitha

Thin Film Center of Excellence, Department of Applied Science, PSG College of Technology, Peelamedu, Coimbatore 641004, Tamil Nadu, India

ARTICLE INFO

Article history:
Received 23 May 2016
Received in revised form 16 August 2016
Accepted 17 August 2016
Available online 22 August 2016

Keywords:
Cotton cellulose
Microwave argon plasma
Process parameter optimization
Box–Behnken design
ATR-FTIR
XRD/FESEM analysis

ABSTRACT

Cotton fabric was processed with microwave (Ar) plasma to alter its hydrophilicity. The process parameters namely microwave power, process gas pressure and processing time were optimized using Box-Behnken method available in the Design Expert software. It was observed that certain combinations of process parameters improved existing hydrophilicity while the other combinations decreased it. ATR-FTIR spectral analysis was used to identify the strain induced in inter chain, intra chain, and inter sheet hydrogen bond and glycosidic covalent bond due to plasma treatment. X-ray diffraction (XRD) studies was used to analyze the effect of plasma on unit cell parameters and degree of crystallinity. Fabric surface etching was identified using FESEM analysis. Thus, it can be concluded that the increase/decrease in the hydrophilicity of the plasma treated fabric was due to these structural and physical changes.

1. Introduction

Box–Behnken method in the Design Expert Software is a process optimization software that is used to optimize the output surface response which is influenced by various independent input parameters. The geometry of this design suggests a sphere within the process space such that the surface of the sphere protrudes through each face with the surface of the sphere tangential to the midpoint of each edge of the space (Aslan & Cebeci, 2007). In this work, this software was used to analyze the effect of microwave argon (Ar) plasma on the hydrophilicity of cotton fabric. The output surface response in the study was wicking height and the input parameters were process gas pressure, microwave power in terms of power percentage and exposure time. Plasma processing of a textile material is one of the effective method to modify its surface properties as per a certain application's requirement (Bengi, Aysun, & Mehmet, 2009; Lia, Zhanga, & Zoua 2015; Porntapin, Meshaya, Worawan, Boonchoat, & Suda, 2016). As the plasma contains energetic particles and the temperature is little higher than the ambient temperature, this cold plasma has the capability to interact with the surface to alter its physio-chemical properties by breaking the cellulose chain, introducing new functional groups and etching the surface. Several plasma sources like DC, RF, DBD, corona and microwave using variety of gases like air, oxygen, argon, helium, hydrogen, fluorinated gas etc., have been used to achieve different types of modifications (Vaideki, Jayakumar, & Rajendran, 2009; Kan & Yuen, 2006; McCord, Hwang, Qiu, Hughes, & Bourham, 2003). Each type of plasma has its own advantages and limitations. Unlike other sources, the striking advantage of microwave assisted plasma source is its very short treatment time. Abidi and Hequet (2005) and Hochart, De Jaeger, and Levalois-Grutzmacher (2003) have successfully converted an inert cotton surface to a reactive one using microwave plasma for further graft polymerization of polymers and also have confirmed the durability of the grafting. Thus the success of plasma treatment lies in the changes induced in structure, crystallinity and morphology of cotton surface.

Nishiyama, Langan, and Chanzy (2002) had reported the changes in the IR spectra of crystalline cellulose Iβ with temperature. The shifts in O—H stretching region were studied in detail to understand the structural changes in cellulose. In the same work, they had also reported about the changes induced by mechanical effects. The effect of tensile load on the inter and intra molecular hydrogen bonds and C—O—C glycosidic bond and in turn its effect on the change in the unit cell parameters and monoclinic angle of the cellulose structure was reported by Altaner, Thomas, Fernandes, and Jarvis (2014b). The thermal and/or mechanical effects can result in the shift in IR frequency pertaining to hydrogen bonds due to a change in the distance between donor and acceptor atoms that are involved in the hydrogen bond. These effects lead to

* Corresponding author.
E-mail addresses: csp@phy.psgtech.ac.in (S. Prabhu), vaideki.krishnakumar@gmail.com (K. Vaideki), vp.anitha@gmail.com (S. Anitha).

http://dx.doi.org/10.1016/j.carbpol.2016.08.057
0144-8617/

changes in bond angle and bond strength and hence bond length between donor and hydrogen atoms (A—H) and between acceptor and hydrogen atoms (H···B) (Jeffrey, 1997). Abidi and Hequet (2004) had reported the generation of reactive carbonyl radicals on the cotton fabric surface due to microwave plasma treatment. The generation of such radicals can in turn affect the hydrogen bonding system and hence the crystallinity of cellulose structure. An increase in crystallinity of the cellulose structure would lead to a strong hydrogen bond network thus reducing the number of accessible hydroxyl groups and vice versa which in turn affects the hydrophilicity of the fabric (Anitha, Vaideki, Jayakumar, Nithya, & Rajendran, 2011). In this work, an attempt has been made to find out the reasons for the changes in hydrophilicity of the cotton fabric due to plasma treatment by analyzing the IR spectrum, X-ray diffraction pattern and FESEM micrographs of the samples. The notable feature of this work is that the existing wettability of cotton fabric has been either improved or impaired to achieve either a highly hydrophilic or non – wettable fabric using a single microwave argon plasma treatment just by altering the process parameters. However, the durability of the surface reactivity is not dealt with in this paper. This would be addressed in the next work.

2. Materials and methods

2.1. Materials

100% pure finished cotton fabric with EPI/PPI ratio of 130/140 was immersed in boiling water for about 1 h. to remove the starch. Fabric samples of width 11 cm and length 17 cm was used for plasma treatment.

2.2. Microwave Ar plasma treatment

Plasma process chamber was a hollow quartz tube of volume: 2521 cm^3, height: 25.1 cm and inner diameter: 14.50 cm. Fabric sample of size 11 cm × 17 cm was suspended at the center of the chamber using a Teflon covered hook. The microwave was generated using a pair of magnetrons. The maximum power that could be given as input to the magnetron pair was 2.2 kW. Prior to the plasma treatment, the chamber was maintained at a base pressure of 6.3×10^{-3} mbar, and subsequently Ar gas was purged into the chamber for 2 min to fill the chamber. The maximum and minimum ranges of the three process parameters viz: operating gas pressure (Pr), power percentage (PP) and exposure time (Et) was fixed as 0.2 mbar–1.5 mbar, 52%–54% of 2.2 kW and 30 s to 270 s respectively. The range of Pr and PP were selected based on the generation of sustained plasma. For the combinations of Pr and PP chosen, plasma treatment less than 30 s did not significantly alter the hydrophilicity of the fabric sample. However, when the sample was immersed in plasma beyond 270 s the fabric samples was charred. Hence the range of Et was selected as mention above. The fabric sample was subjected to all tests immediately after the plasma treatment.

2.3. Model development

Box–Behnken model (Design Expert software v7.0.0, Stat Ease Inc., Minneapolis, USA) was used in this work to optimize output surface response with respect to the input process parameters. The output response in this study was the wicking height. Combinations of experimental runs suggested by the model in terms of coded and actual variables are presented in Table 1.Where,

Table 1
Combinations of input variable parameters.

		Coded Variables			Actual Variables		
Std	Run	A	B	C	Pr	Et	PP
2	1	+1	−1	0	1.5	30	53
3	2	−1	+1	0	0.2	270	53
4	3	+1	+1	0	1.5	270	53
12	4	0	+1	+1	0.85	270	54
15	5	0	0	0	0.85	150	53
9	6	0	−1	−1	0.85	30	52
7	7	−1	0	+1	0.2	150	54
10	8	0	+1	−1	0.85	270	52
8	9	+1	0	+1	1.5	150	54
1	10	−1	−1	0	0.2	30	53
11	11	0	−1	+1	0.85	30	54
14	12	0	0	0	0.85	150	53
5	13	−1	0	−1	0.2	150	52
6	14	+1	0	−1	1.5	150	52
13	15	0	0	0	0.85	150	53

$$\left.\begin{aligned} A &= (Pr - 0.85)/0.65 \\ B &= (Et - 150)/120 \\ C &= (PP - 53)/1 \end{aligned}\right\} \quad (1)$$

The repeatability of the study was taken care in this model which is reflected in Table 1 as run number 5, 12 and 15.

2.4. Assessment of hydrophilicity

Wicking and wetting ability of the cotton sample was used as a measure of hydrophilicity

2.4.1. Wicking test (AATCC test method 197-2013)

The spontaneous flow of water in the fabric pores due to capillary action and the subsequent reaction between free hydroxyl groups in cellulose and water molecule gives the wicking ability for cotton fabric. The sample was cut into 5 strips of 2 cm × 14 cm and was suspended vertically. The end of the strip was kept on the surface of the water reservoir in a 250 ml beaker. The wicking height of the strip was measured for every 10 s for first 5 min, after which it was measured for every 1 min up to 10 min. Thereafter the wicking height was measured for every 5 min upto 45th min. The average wicking height at the end of 45 min was considered as wicking height of the sample (Saville, 2002).

2.4.2. Wettability test (BS 4554-1970)

The treated and untreated cotton fabric was tested for its wettability as per BS 4554-1970 method. The fabric was kept taut and placed in horizontal position. Clean burette filled with double distilled water was kept at a distance of 6 mm from the fabric surface. The tip of the burette was 1.22 mm in diameter. A droplet of water was allowed to fall on the taut sample surface. The spot light was kept at 45° with respect to the fabric surface at a distance of 250 mm and the reflection of the light was viewed at an angle of 45° from the opposite side of the spot light. The duration of time taken by the droplet to disappear was noted as sample's wetting time (Saville, 2002).

2.4.3. Water repellency: spray test (AATCC test method 22-2015)

The water repellency character of the cotton fabric was assessed by means of spray rating using spray test method (Saville, 2002). The spraying funnel of height 200 ± 10 mm was calibrated by pouring 250 ml of distilled water into it and adjusting the spray time between 25 and 30 s by enlarging or blocking the nozzle size at the

Table 2
Response to the respective experimental runs.

Run	Factor 1 (Pr) A: Pressure (mbar)	Factor 2 (Et) B: Time (s)	Factor 3 (PP) C: Power (%)	Response 1 Wicking Height (cm)
1	1.50	30	53	1.6
2	0.20	270	53	11.92
3	1.50	270	53	4.02
4	0.85	270	54	9.4
5	0.85	150	53	9.8
6	0.85	30	52	5.18
7	0.20	150	54	0.94
8	0.85	270	52	10.06
9	1.50	150	54	2.68
10	0.20	30	53	1.16
11	0.85	30	54	2.48
12	0.85	150	53	8.94
13	0.20	150	52	9.38
14	1.50	150	52	0.9
15	0.85	150	53	8.04

bottom of the funnel. The test sample was kept taut at an angle of 45° facing the funnel nozzle separated by a distance of 150 ± 2 mm. 250 ml of water was poured into the funnel with the test sample below and water was allowed to spray on sample for 25–30 s. After spraying, the opposite side of the sample was tapped to remove the water droplets on the surface of the sample and the wet pattern was compared with the standard rating chart.

2.4.4. Mean pore radius determination

As the wicking height depends on mean pore radius for a multipores material, it was calculated using modified Washburn's equation given below in Eq. (2).

$$L^2 = \frac{\gamma D t}{4\eta} \tag{2}$$

Where,
L → wicking height
γ → Surface tension of water
D → Mean Pore radius
t → Time taken to reach the height L
η → Viscosity of water

2.5. Characterization of argon plasma treated sample

2.5.1. X-ray diffraction analysis

The X-ray diffraction pattern of the sample was acquired using Schimadzu, Japan/600 diffractometer. The CuKα radiation source of wavelength 1.54060 Å was used for getting the pattern. The lattice parameters and percentage crystallinity index of the samples were calculated using Eqs. (3) and (4) respectively.

$$\frac{1}{d^2} = \frac{1}{sin^2\beta}\left[\frac{h^2}{a^2} + \frac{k^2 sin^2\beta}{b^2} + \frac{l^2}{c^2} - \frac{2hlcos\beta}{ac}\right] \tag{3}$$

Where,
d → d – spacing
h, k, l → lattice planes
a, b, c → crystallographic axis
β → crystallographic angle

$$CI = \frac{I_{(002)} - I_{(amp)}}{I_{(002)}} \times 100 \tag{4}$$

Where,
CI → Crystallinity Index
$I_{(002)}$ → Maximum intensity of the crystalline cellulose peak ($2\theta = 22.7°$)
$I_{(amp)}$ → Maximum intensity of the amorphous cellulose peak ($2\theta = 18.0°$)

2.5.2. Attenuated total reflectance fourier transform infra-Red (ATR-FTIR) spectral analysis

The ATR-FTIR spectrum of the sample was acquired using FTIR spectrometer (Perkin Elmer, USA, Spectrum Two). The spectrum was directly collected from the sample using Zinc Selenide (ZnSe) plate without any special preparation. The resolution of the equipment was 4 cm^{-1} with 64 scans and the spectra were obtained within the window of 4000 cm^{-1}–500 cm^{-1}.

2.5.3. Field emission scanning electron microscope (FESEM)

The surface morphology of the sample was analyzed using FESEM (Carl Zeiss, UK, SIGMA). The non – conductive sample was given conductive gold coating. The magnification used in the current study was 20,000 x.

3. Result and discussion

3.1. Box–Behnken Analysis

The wicking height at the end of 45 min was given as response to the respective experimental runs suggested by the design (Table 2).

Based on the response, the design suggested quadratic model as the best fit. Table 3 gives the sequential sum of squares for available models. The F-value indicates significance of adding new terms to the existing model while p-value indicates the improvement of model due to the additional terms.

For a model to be significant F and p value should be highest and lowest respectively and in the present case quadratic model satisfies the condition.

Table 4 presents the data pertaining to lack of fit test. The F value compares the variation of the difference between the average response at a design point and the corresponding estimated response with pure error while the p-value indicates the presence of some residual terms in the model.

For the model to have a best fit for the input data the F value should be lowest and p value should be greater than 0.1. On this basis too, the quadratic is the best to mathematically model the response.

Standard deviation (Std. Dev.) of the design error, correlation coefficient (R - Squared) and Predicted Residual Error Sum of Squares (PRESS) are the other statistical parameters that have to be compared to decide upon the best model. The comparative data are presented in Table 5.

Table 3
Sequential Models.

Source	Sum of Squares	df	Mean Square	F Value	p – valueProb > F	
Mean vs. Total	498.82	1	498.82			
Linear vs. Mean	115.76	3	38.59	3.94	0.0391	
2FI vs. Linear	44.45	3	14.85	1.88	0.2107	
Quadratic vs. 2FI	59.84	3	19.95	31.04	0.0012	Suggested
Cubic vs. Quadra	1.66	3	0.55	0.72	0.6273	Aliased
Residual	1.55	2	0.77			
Total	722.16	15	48.14			

Table 4
Lack of Fit.

Source	Sum of Squares	df	Mean Square	F Value	p – valueProb > F	
Linear	106.04	9	11.78	15.21	0.0632	
2FI	61.50	6	10.25	13.23	0.0719	
Quadratic	1.66	3	0.55	0.72	0.6273	Suggested
Cubic	0.000	0				Aliased
Pure Error	1.55	2	0.77			

Table 5
Model Summary Statistics.

Source	Std. Dev.	R – Squared	AdjustedR – Squared	PredictedR – Squared	PRESS	
Linear	3.13	0.5183	0.9869	0.1085	199.11	
2FI	2.81	0.7177	0.5060	0.0859	204.16	
Quadratic	0.80	0.9856	0.9597	0.8652	30.11	Suggested
Cubic	0.88	0.9931	0.9515		+	Aliased

+ Case(s) with leverage of 1.0000: PRESS statistic not defined.

Table 6
ANOVA for response Surface.

Source	Sum of squares	df	Mean Square	F Value	P – valueProb > F	
Model	220.13	9	24.46	38.06	0.0004	Significant
A – Pressure	25.21	1	25.21	39.22	0.0015	Significant
B – Time	78.00	1	78.00	121.38	0.0001	Significant
C – Power	12.55	1	12.55	19.53	0.0069	Significant
AB	17.39	1	17.39	27.06	0.0035	Significant
AC	26.11	1	26.11	40.63	0.0014	Significant
BC	1.04	1	1.04	1.62	0.2592	Not Significant
A^2	52.71	1	52.71	82.02	0.0003	Significant
B^2	0.83	1	0.83	1.29	0.3080	Not Significant
C^2	10.34	1	10.34	16.09	0.0120	Significant
Residual	3.21	5	0.64			
Lack of Fit	1.66	3	0.55	0.72	0.6273	Not Significant
Pure Error	1.55	2	0.77			
Cor Total	223.35	14				

The best model for the observed response would be the one that has a minimal Standard Std. Dev., R - Squared values close to 1.0 and PRESS value the lowest. From Table 5 it is evident that quadratic model satisfies the mentioned conditions.

The ANOVA for Response Surface Quadratic Model by the Box–Behnken design is given in Table 6.

F value in Table 6 compares the variance of each term with error variance. If the term has an influence on the response, the ratio between the two will not be close to 1. The p value associated with F value is actually the probability of obtaining the respective term's F value and it should be less than 0.05 for the term to be significant. Hence, from Table 6, the terms A, B, C, AB, AC, A^2 and C^2 are the significant model terms. The equation for the quadratic model with coded factors and actual factors suggested by the design is given in Eqs. (5) and (6) respectively.

$$\text{Wicking height} = +8.93 - 1.78 * A + 3.12 * B - 1.25 * C - 2.09 * A * B + 2.56 * A * C + 0.51 * B * C - 3.78 * A^2 - 0.47 * B^2 - 1.67 * C^2 \quad (5)$$

$$\text{Wicking height} = -4426.40641 - 191.84916 * Pr - 0.16665 * Et + 172.14218 * PP - 0.026731 * Pr * Et + 3.93077 * Pr * PP + 4.25000E - 003 * Et * PP - 8.94280 * Pr^2 - 3.28704E - 005 * Et^2 - 1.67333 * PP^2 \quad (6)$$

As per Eq. (6), the wicking response predicted by the design for the design points, the actual response and the residual term are shown in Fig. 1.

It is evident from Fig. 1, that the residual term is small. The effect of terms in Eq. (1) that have a significant influence on the wicking response as suggested by the Box–Behnken design are presented in Figs. 2 and 3.

Fig. 2a shows that for a constant power percentage of 54% and exposure time of 150 s, the wicking height increased from 0.94 cm to 6.00 cm for a variation in gas pressure from 0.2 to 0.89 mbar and decreased thereafter and reduced to 2.68 cm at 1.5 mbar. In a similar manner, for other combinations of constant power percentage and exposure time, the wicking height followed the same trend within the gas pressure rage shown in Fig. 2a. However, the highest wicking height of 13.28 cm was observed for a combination of a gas pressure: 0.2 mbar, power percentage: 52% and exposure time: 270 s. The variation in wicking height with respect to power percentage for a constant gas pressure and exposure time also exhibited similar trend (Fig. 2c).

Fig. 2b explains the influence of exposure time on wicking response at a constant gas pressure and power percentage. For a constant gas pressure and power percentage of 0.85 mbar and 54% respectively, as the exposure time varied from 30 s to 270 s, the wicking response increased linearly from 1.89 cm to 9.16 cm. Here too, interestingly for any combination of gas pressure and power percentage, the wicking height increased linearly with time. The effect of two factors on wicking height i.e., AB (Pr*Et) and AC (Pr*PP) is presented in Fig. 3a and b.

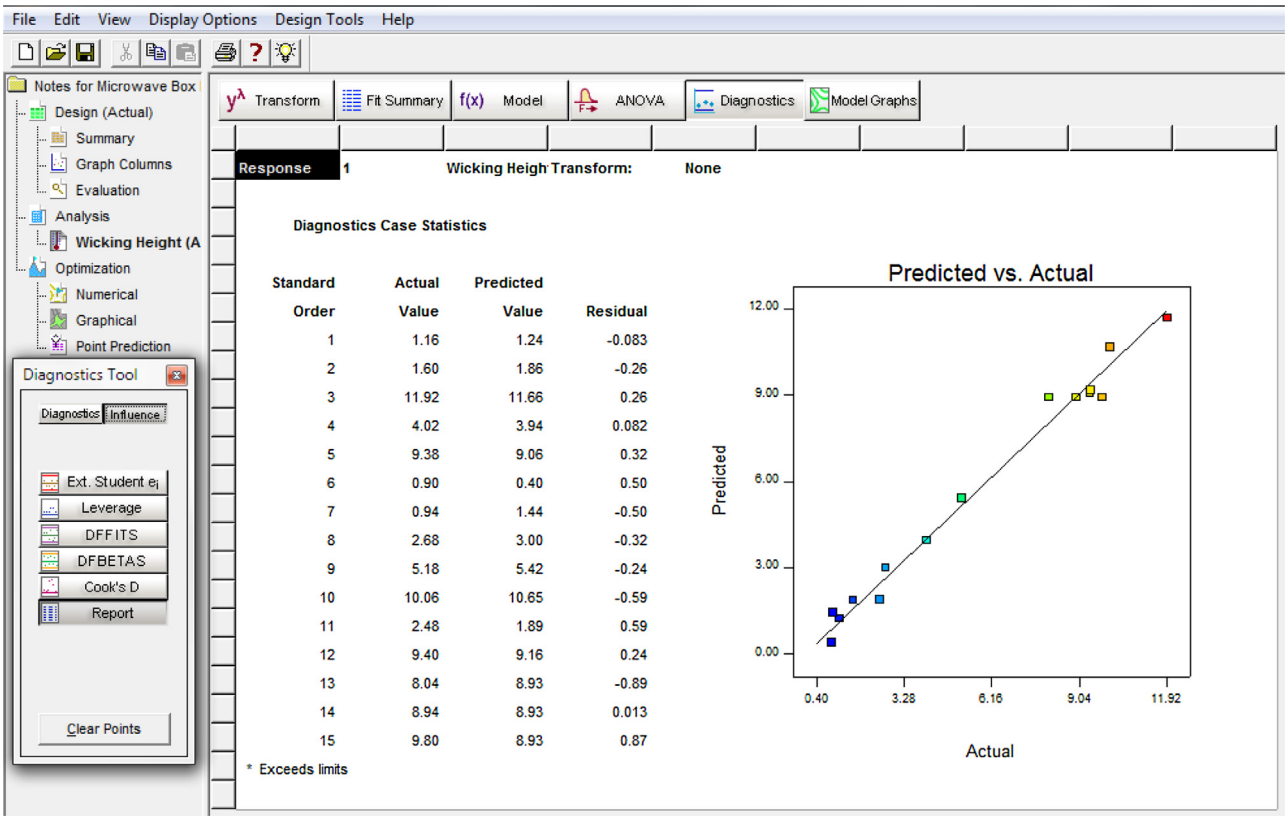

Fig. 1. Diagnostics of the experimental runs.

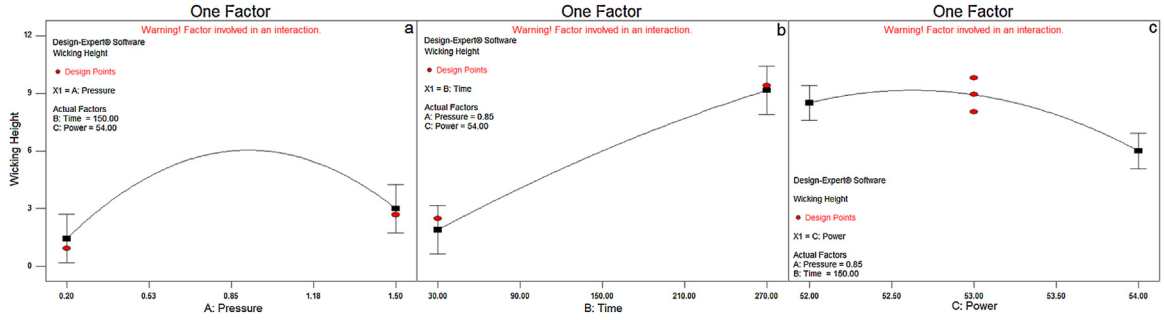

Fig. 2. One factor interaction: Effect of (a) gas pressure (b) exposure time and (c) power percentage on wicking height.

3.2. Optimization of process parameters

The mean wicking height of the untreated cotton fabric (control) was observed to be 9.68 cm. Table 2 clearly reveals the fact that the hydrophilicity of the cotton fabric was either improved or impaired based on the combination of process parameters used during plasma treatment. Hence, it was decided to optimize the process parameters to achieve both improved hydrophilic and impaired hydrophilic (non-wetting) property. The software suggested best thirty combinations each to obtain improved hydrophilic and impaired hydrophilic character for which the desirability is one. Two combinations from this list one each for hydrophilic and impaired hydrophilic property were tested. The sample treated at a gas pressure of 0.38 mbar, power percentage of 52.15% and exposure time of 264.87 s exhibited an average wicking height of 13.16 cm which is a 36% increase in wicking height when compared to the control sample. Whereas, the sample treated at a gas pressure of 0.20 mbar, power percentage of 53.93% and exposure time of 35.94 s did not exhibit wicking property which was in correlation with the theoretical value of −4.00 cm as predicted by the quadratic equation. Since, the wetting ability of the treated samples seemed to show both improved and impaired hydrophilic nature, it can be understood that there was a change in surface energy of the samples. The surface energy of the fabric before and after plasma treatment was determined using Zismann plot. 6.0 M NaCl solution, 5.0 M NaCl solution, Double Distilled Water (D. D Water), 1 ml (DMSO): 9 ml (D. D. Water) and 3 ml (DMSO): 7 ml (D. D. Water) of surface tension 82.25 mN/m, 78.49 mN/m, 72.00 mN/m, 61.53 mN/m and 57.91 mN/m at 30° respectively, were used for this study. The surface energy of the control fabric and that of non-wetting fabric was found to be 45.45 mN/m and 28.28 mN/m respectively. Whereas all the liquids tend to wet the hydrophilic fabric surface instantaneously which indicated an increase in surface energy >82.55 mN/m. Fig. 4 is an evidence of the observed changes in surface energy for the fabric before and after plasma treatment.

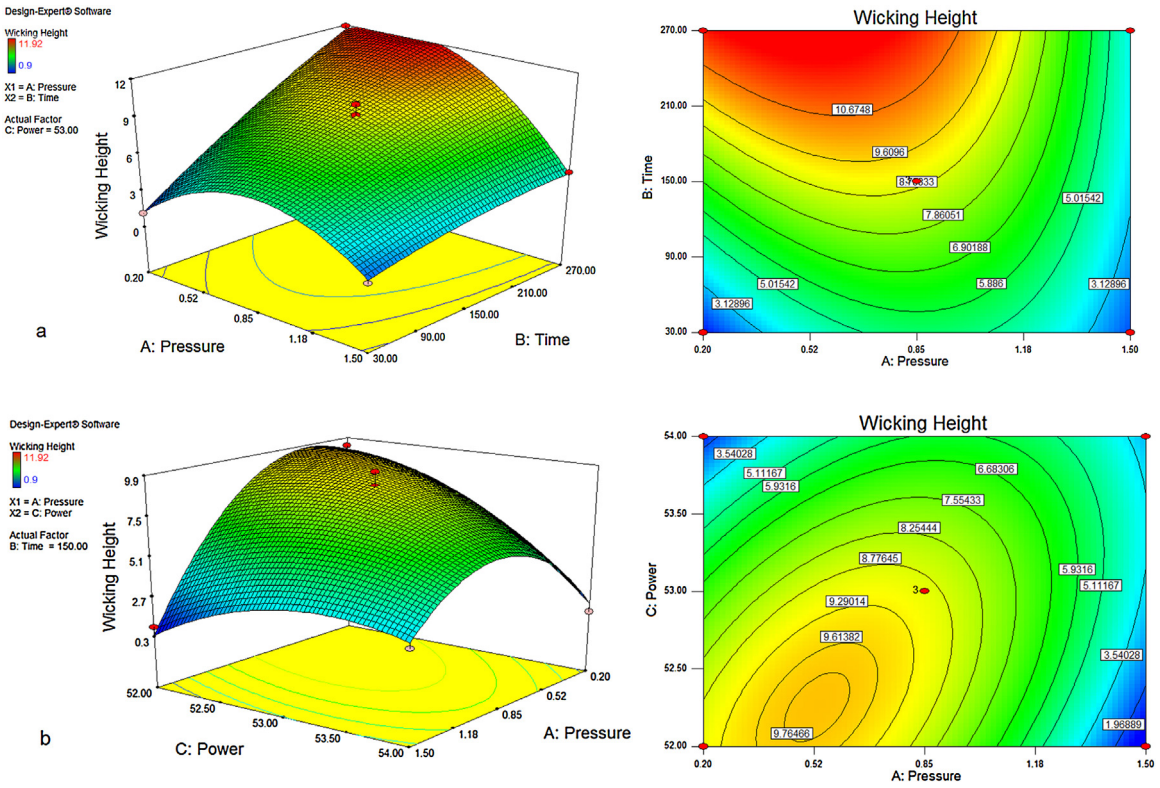

Fig. 3. 3D Surface and contour plot of simultaneous variation of gas pressure (a) and exposure time vs wicking response (b) and power percentage vs wicking response.

The hydrophobic response of the sample was assessed using spray test and it was observed that the standard spray test rating was 70 (ISO 2) which referred to the partial wetting of the sample face beyond the spray points. The reason for all these observations was analyzed using ATR − FTIR, XRD and FESEM studies.

3.3. ATR-FTIR analysis

The two samples that exhibited maximum (MaxWH) and minimum (MinWH) wickability were subjected to IR analysis. The ATR-FTIR spectrum of the two samples was taken prior to and immediately after the plasma treatment in a marked region of the fabric so as to analyze what exactly has happened during the plasma treatment. The two comparative spectra are presented in Fig. 5a and 5b.

Fig. 5a shows a shift in the following IR absorption frequencies of the plasma treated sample that exhibited maximum wicking when compared to the control. The convention followed in the present study is that the cellulose chain is considered to be present along the b-axis of the unit cell. The peak at 3260 cm^{-1} corresponding to O6—H stretching (str) oriented transverse to the axis of the cellulose chain, is shifted to 3256 cm^{-1} after plasma treatment that indicated a decrease in bond energy and hence an increase in bond length. Also, the peak at 2953 cm^{-1} and 2894 cm^{-1} assigned to asymmetric and symmetric C6—H_2 str (Altaner, Horikawa, Sugiyama, & Jarvis, 2014a) was shifted towards lower frequency representing an elongation with respect to C6—H covalent bond which in turn rotated C_6 and could possibly result in a rotation about C_5—C_6 covalent bond (Altaner et al., 2014b). The combined effect of the changes in the respective vibrations could result in changes in O6H···O3 intermolecular hydrogen bond length (Altaner et al., 2014b; Nishiyama et al., 2002). Since, this is present along the a-axis of the cellulose unit cell, the XRD analysis could throw more light on this change. Similarly, a shift in 3357 cm^{-1} (O3—H str) and 3467 cm^{-1} (O2—H str) to 3372 cm^{-1} and 3474 cm^{-1} respectively indicated lengthening of the O3H···O5 and O2H···O6 intramolecular hydrogen bond (Altaner et al., 2014b; Nishiyama et al., 2002). Also, the C—O—C glycosidic asymmetric vibration band at 1157 cm^{-1} did not shift indicating that there was no shortening or elongation of the bond length (Altaner et al., 2014b). These observations showed that the lengthening of the flanking hydrogen bond and rotation about C_5—C_6 covalent bond with no change in the C—O—C glycosidic covalent bond length, would result in a ring stretch that would cause a change in the b- axis of the unit cell. The peak at 2919 cm^{-1} and 2851 cm^{-1} representing ring C—H str (Altaner et al., 2014a) vibrations is shifted to lower frequencies after plasma treatment which indicated weakening of C—H covalent bond and strengthening of the inter sheet C—H···O bond that would reflect as a change in the c-axis dimension of the unit cell.

The comparison between ATR-FTIR spectra of the control sample and the one that exhibited minimum wickability is shown in Fig. 5b. The shift in peak at 3261 cm^{-1}–3258 cm^{-1} and asymmetric and symmetric C6—H_2 str towards lower frequency after plasma treatment represented shortening of O6—H bond and rotation about C_6—C_5 bond, disclosing a change in the O6H ··· O3 inter molecular hydrogen bond length. The shift in bands at 3360 cm^{-1} and 3468 cm^{-1} to 3358 cm^{-1} and 3470 cm^{-1} respectively indicated shortening and lengthening of O3H···O5 and O2H···O6 intramolecular hydrogen bond respectively. The peak at 1157 cm^{-1} shifted to 1159 cm^{-1} indicating shortening of C—O—C glycosidic bond unlike the previous case. From these observations it can be concluded that during this particular plasma treatment, the lengthening and rotation of the O2H···O6 flanking hydrogen bond and C_5—C_6 covalent bond, is being resisted by the shortening of the O3H···O5 intramolecular hydrogen bond and C—O—C glycosidic covalent bond. Also, the red shift in the peaks corresponding to C—H str vibrations leads to a change in the weak inter sheet C—H···O bond length. These overall changes caused a strain in the cellulose unit cell.

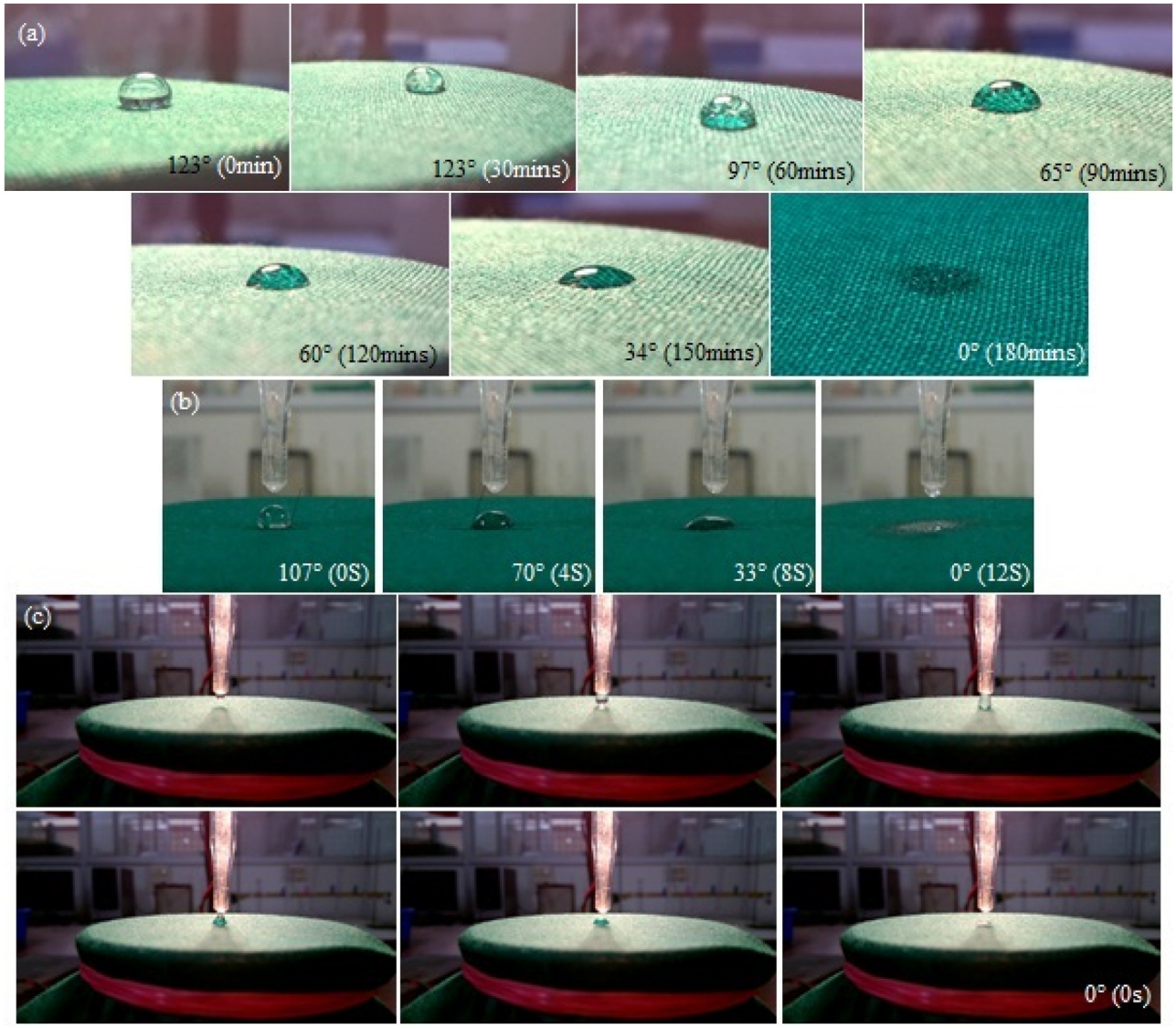

Fig. 4. Water Contact angle (a) sample with impaired hydrophilicity (b) control and (c) sample with improved hydrophilicity.

In both the cases, shift in the other peaks present in the spectra was not observed except for a small change in the intensity of their absorbance. Pictorial representations of cellulose structure along with inter and intra molecular hydrogen bond is shown in Fig. 6a. The changes that occurred after plasma treatment in both the cases are presented in Fig. 6b and 6c.

3.4. XRD analysis

The changes in the cellulose unit cell of the two samples after plasma treatment as indicated by the ATR-FTIR spectral analysis was ascertained by comparing the XRD patterns (Fig. 7) of the control sample with that of the two plasma treated samples. The crystallographic axes of the Native cellulose are a = 7.784 Å, b = 8.201 Å, c = 10.38 Å and β = 96.5° (Nishiyama et al., 2002).

It can be observed from Table 7 that the lattice parameters of the unit cell have been altered significantly after the plasma treatment which was calculated using Eq. (3). The change in values of crystallographic axis 'a', 'b' and 'c' and crystallographic angle 'β' was calculated using the reflections from (0 0 2), (0 4 0), (ī 0 1) and (1 0 1) planes.

Table 7
Crystallinity index and lattice parameters of the samples.

Sample Parameters	Control	MaxWH	MinWH
a (Å)	7.72	8.04	7.46
b (Å)	10.20	10.32	10.28
c (Å)	7.66	7.64	7.77
β (°)	93.92	95.07	92.77
[a]d (c/2) (Å)	3.83	3.82	3.885
Crystallinity Index (%)	69.85	67.32	71.52

[a] d is the distance between two cellulose sheets.

The Table 7 shows an increase in the unit cell parameters of the sample that exhibited maximum wicking along 'a' and 'b' axis when compared to the control sample and almost no change along the c-axis. The 4.15% increase in dimension along a-axis is attributed to the increase in the O6H···O3 intermolecular hydrogen bond length due to lengthening O6—H bond and rotation of C_5—C_6 covalent bond. The 1.18% increase in the 'b' axis is ascribed to the ring stretch due to the lengthening of the flanking hydrogen bond and rotation about C_5—C_6 covalent bond with no change in the C—O—C glycosidic bond length. Since, there was no significant change (a

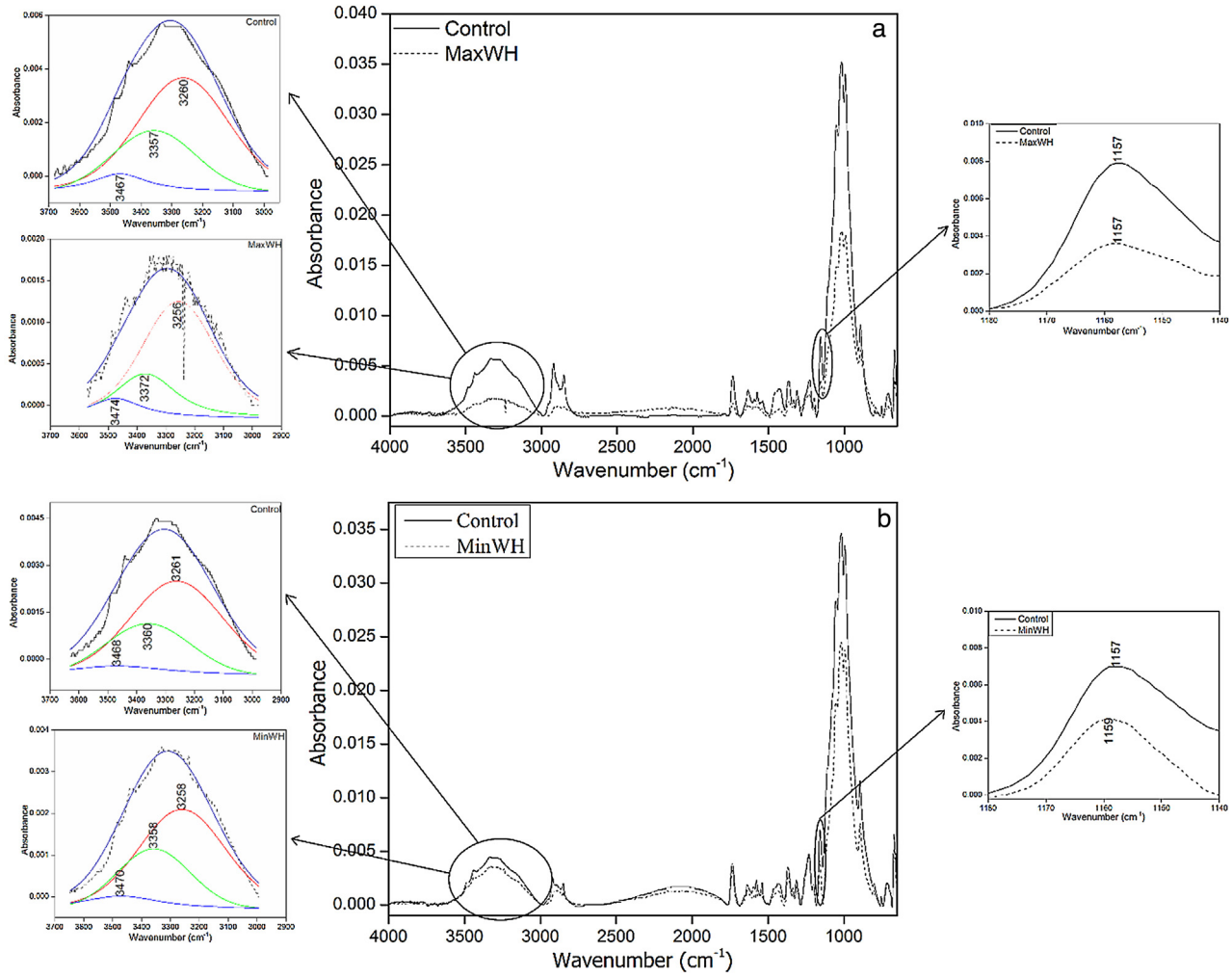

Fig. 5. ATR-FTIR spectrum of (a) control vs MaxWH sample (b) control vs MinWH sample.

0.26% decrease) along the c-axis, it can be inferred that there was no appreciable change in the week C—H···O inter sheet hydrogen bonds. The monoclinic angle increased when compared to control sample due to the overall strain in the unit cell. Table 7 also indicated the decrease in crystallinity index of the plasma treated sample. This may be attributed to the weakening of the intra and inter molecular hydrogen bond which may eventually break leading to a disordered arrangement of cellulose chain. This would in turn give rise to free hydroxyl groups thereby improving the hydrophilicity of the sample.

Comparing the XRD data of the control and the sample that exhibited minimum wicking, there is a 3.49% decrease in a-axis which is attributed to the shortening of the O6H···O3 intermolecular hydrogen bond length due to shortening of O6—H bond and rotation of C_5—C_6 covalent bond. The small 0.78% increase in the b-axis of the unit cell is attributed to shortening and lengthening of O3H···O5 and O2H···O6 intramolecular hydrogen bond respectively and shortening of C—O—C glycosidic bond. The, 1.44% increase in the c-axis is attributed to the increase in the inter sheet hydrogen bond and all these overall changes has resulted in a decrease in the monoclinic angle. The strains induced in the cellulose structure seems to have promoted further inter and intra molecular hydrogen bonds which is reflected as an increase in the crystallinity index when compared to control sample, leading to a decrease in the free hydroxyl group and hence a decrease in the hydrophilicity.

Table 8
Mean pore radius of the samples.

Sample	Mean Pore radius (μm)
Control sample	0.199
MaxWH	0.311
MinWH	–

3.5. FESEM analysis and mean pore radius

The mean pore radius of the control and MaxWH samples was calculated using Modified Washburn Equation given in Eq. (4) and the values are given in Table 8. Since the MinWH sample, was not able to wick water, it was not possible to calculate its mean pore radius.

From the data in Table 8 it is a clear that the plasma treatment not only induces chemical and structural changes but also physical changes on the sample surface. The appreciable difference was due to the etching effect of plasma. To ascertain the results, the samples were subjected to FESEM analysis.

Fig. 8 shows the FESEM images of the three fabric samples. It is clear that the surface of the sample which exhibits maximum wicking is roughened due to plasma etching and thereby creating new pores and widening the existing pores. This improved the capillarity of the fabric. The results obtained are in agreement with the

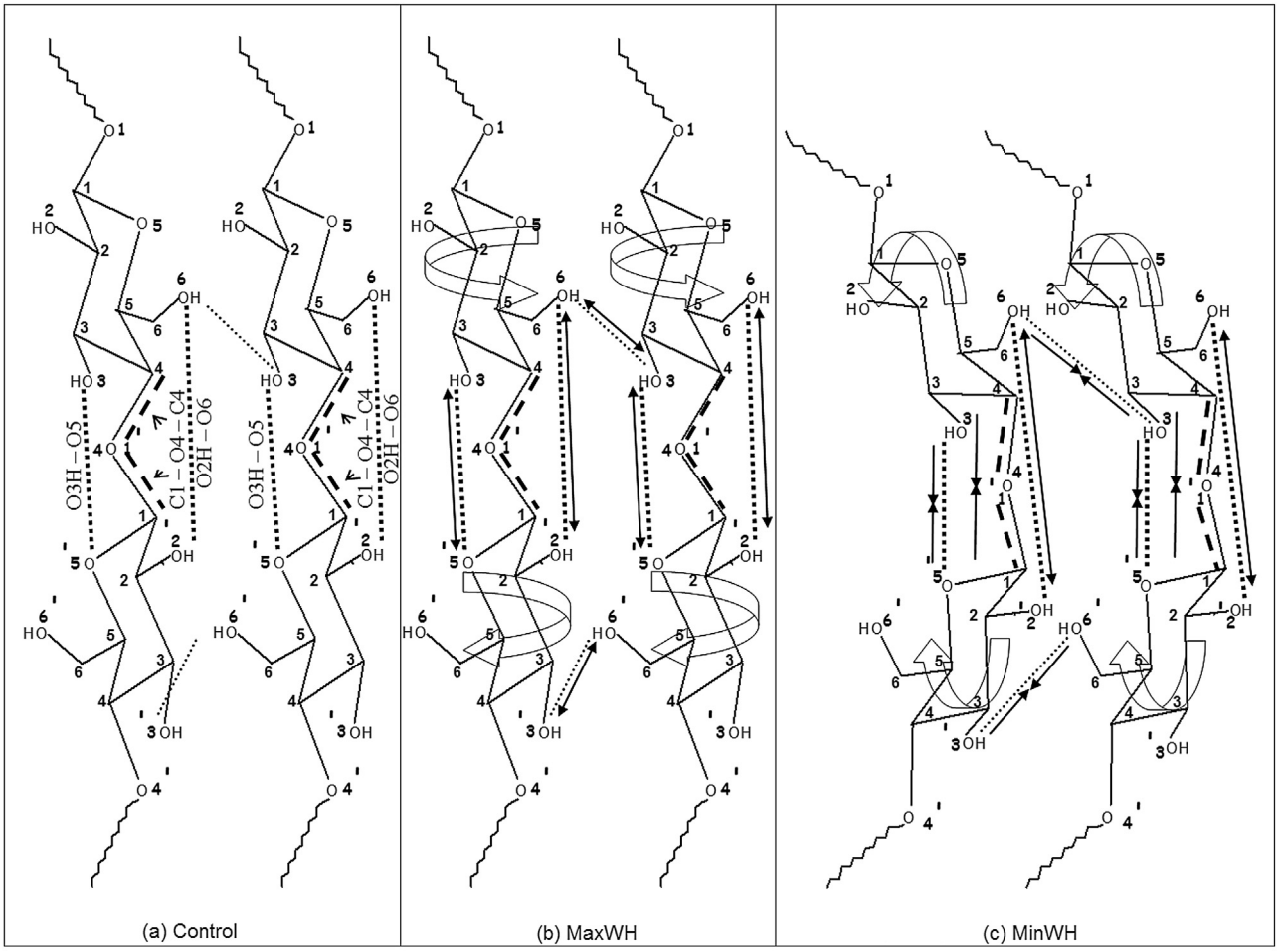

Fig. 6. Structure of (a) Control cellulose (b) MaxWH cellulose (c) MinWH cellulose.

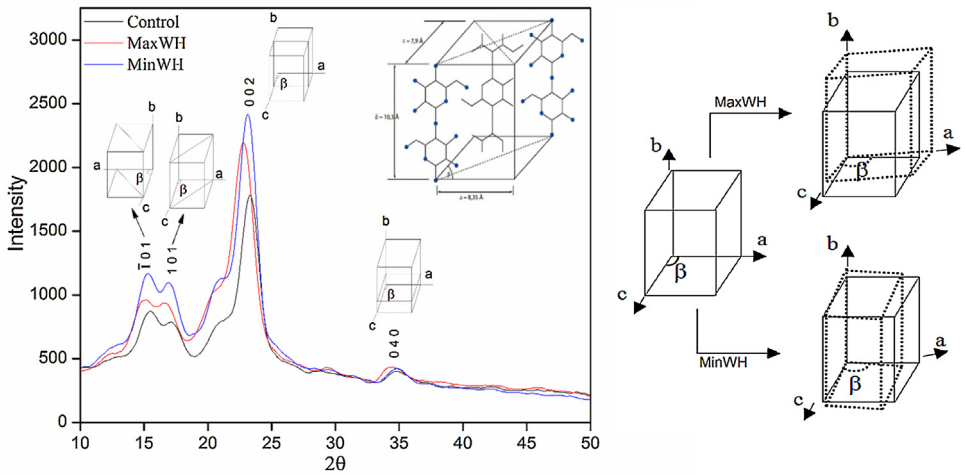

Fig. 7. XRD diffraction pattern and changes in the unit cell of the two plasma treated samples (Insert: Original Meyer and Misch model for cellulose I, with the designation of the axes used in 1937).

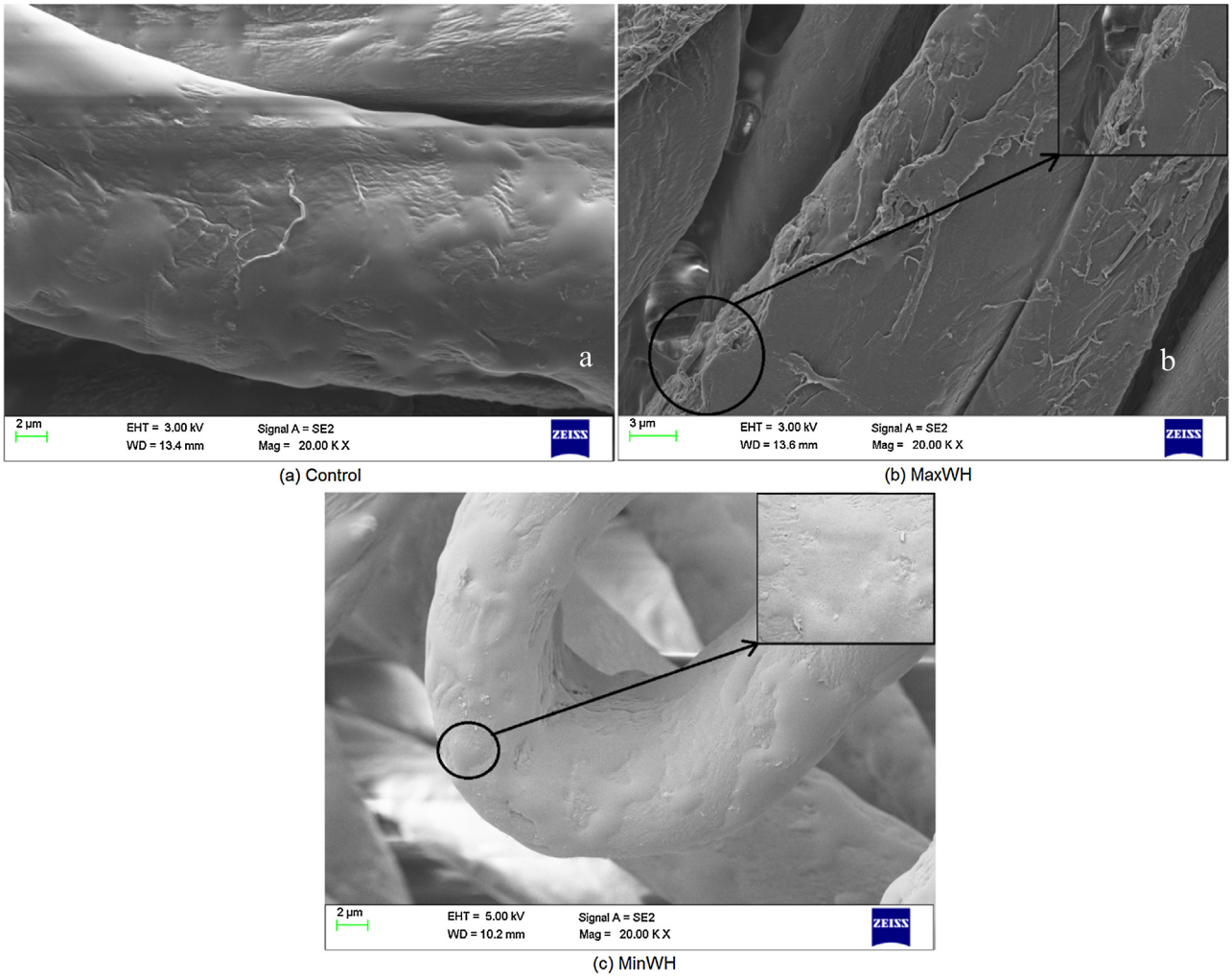

Fig. 8. FESEM images of (a) Control sample (b) MaxWH sample (c) MinWH sample.

work carried out by Navaneetha Pandiyaraj and Selvaraj (2007). Whereas, the surface of the sample that exhibited minimum wicking is smoothened after plasma treatment disclosing the fact that the fibrils on the surface are etched away thereby removing the part of cellulose that contains maximum amorphous region (De Souza, Bouchard, Methot, Berry, & Argyropoulos, 2002) thus reducing the hydrophilicity.

Thus the most striking observation of the present study is, a single microwave Ar plasma processing of the cotton fabric is sufficient to achieve either an improvement or impairment in the hydrophilicity of the fabric just by varying the combination of process parameters because the interaction between energetic particles in the generated plasma and fabric induced both structural and physical changes that are responsible for the observed variations in the hydrophilic property.

4. Conclusions

In this study, the Box–Behnken design constructed to optimize microwave Ar plasma treatment of cotton fabric recommended quadratic model for the input parameters and its response. It was found that the sample treated with minimum gas pressure for maximum exposure time showed hydrophilic nature, whereas the sample treated with maximum gas pressure for minimum power percentage showed hydrophobic nature. From the ATR-FTIR analysis is was found that there were no additional peaks pertaining to new functional groups. It was also found that a sizeable change in the intensities of the IR spectra, and the shift in the IR wave numbers which lead to a strain in the inter, intra molecular and intersheet hydrogen bond and glycosidic linkage of the cellulose chain. XRD study indicated that there was a decrease and increase in the crystallinity of the sample showing hydrophilic and hydrophobic behavior respectively compared to the control sample. In agreement with the increased hydrophilic and reduced hydrophilic nature, the FESEM images show the etching and smoothing of the cellulose fiber compared to the control sample. Hence it can be concluded that using a single plasma treatment dual property can be imparted to cotton fabric just by varying the process parameters.

Acknowledgements

Funding: This work was supported by the Department of Science and Technology (DST), Science and Engineering Research Board (SERB), New Delhi [grant number SB/TP/ETA – 266/2012]. Also authors would like to thank management of PSG College of Technology.

References

Abidi, N., & Hequet, E. (2004). Cotton fabric graft copolymerization using microwave plasma. I. Universal attenuated total reflectance-FTIR study. *Journal of Applied Polymer Science*, *93*, 145–154.

Abidi, N., & Hequet, E. (2005). Cotton fabric graft copolymerization using microwave plasma. II. Physical properties. *Journal of Applied Polymer Science*, *98*, 896–902.
Altaner, C. M., Horikawa, Y., Sugiyama, J., & Jarvis, M. C. (2014). Cellulose Iβ investigated by IR-spectroscopy at low temperatures. *Cellulose*, *21*, 3171–3179.
Altaner, C. M., Thomas, L. H., Fernandes, A. N., & Jarvis, M. C. (2014). How cellulose stretches: Synergism between covalent and hydrogen bonding. *Journal of Bio Macromolecules*, *15*, 791–798.
Anitha, S., Vaideki, K., Jayakumar, S., Nithya, E., & Rajendran, R. (2011). Study on hydrophilicity and anti-microbial efficacy of microwave plasma and neem oil vapor treated cotton fabric. *Energy and Eco Friendly Materials*, 394–400.
Aslan, N., & Cebeci, Y. (2007). Application of Box–Behnken design and response surface methodology for modeling of some Turkish coals. *Journal of Fuel*, *86*, 90–97.
Bengi, K., Aysun, C. A., & Mehmet, M. (2009). Surface modification and characterization of cotton and polyamide fabrics by plasma polymerization of hexamethyldisilane and hexamethyldisiloxane. *International Journal of Clothing Science and Technology*, *21*, 137–145.
De Souza, I. J., Bouchard, J., Méthot, M., Berry, R., & Argyropoulos, D. (2002). Carbohydrates in oxygen delignification: Part I: Changes in cellulose crystallinity. *Journal of Pulp and Paper Science*, *28*, 167–170.
Hochart, F., De Jaeger, R., & Levalois-Grutzmacher, J. (2003). Graft-polymerization of a hydrophobic monomer onto PAN textile by low-pressure plasma treatments. *Surface and Coatings Technology*, *165*, 201–210.
1997 Jeffrey, G. A. (1997). *An introduction to hydrogen bonding: topics in physical chemistry*. New York: Oxford University Press.
Kan, C. W., & Yuen, C. W. M. (2006). Textile modification with plasma treatment. *Research Journal of Textile and Apparel*, *Vol. 10*(1).
Lia, Y., Zhanga, Y., Zoua, C., & Shao, J. (2015). Study of plasma-induced graft polymerization of stearyl methacrylateon cotton fabric substrates. *Applied Surface Science*, *357*, 2327–2332.
McCord, M. G., Hwang, Y. J., Qiu, Y., Hughes, L. K., & Bourham, M. A. (2003). Surface analysis of cotton fabrics fluornated in radio frequency plasma. *Journal of Applied Polymer Science*, *88*, 2038–2047.
Navaneetha Pandiyaraj, K., & Selvaraj, V. (2007). Non-thermal plasma treatment for hydrophilicity improvement of grey cotton fabrics. *Journal of Materials Processing and Technology*, *199*(1–3), 130–139.
Nishiyama, Y., Langan, P., & Chanzy, H. (2002). Crystal structure and hydrogen-bonding system in cellulose Iβ from synchrotron X–ray and neutron fiber diffraction. *Journal American Chemical Society*, *124*, 9074–9082.
Porntapin, P., Meshaya, P., Worawan, B., Boonchoat, P., & Suda, K. (2016). Surface modification of cotton fabrics by gas plasmas for color strength and adhesion by inkjet ink printing. *Applied Surface Science*, *364*, 208–220.
Saville, B. P. (2002). *Physical testing of textiles*. North America: Woodhead Publishing Ltd.
Vaideki, K., Jayakumar, S., & Rajendran, R. (2009). Investigation on the enhancement of antimicrobial activity of neem leaf extract treated cotton fabric using DC air and oxygen plasma. *Plasma Chemistry and Plasma Processing*, *29*, 515–534.